PAR_2 activation alters colonic paracellular permeability in mice via IFN-γ-dependent and -independent pathways

Nicolas Cenac[1], Alex C. Chin[3], Rafael Garcia-Villar[1], Christel Salvador-Cartier[1], Laurent Ferrier[1], Nathalie Vergnolle[2], André G. Buret[3], Jean Fioramonti[1] and Lionel Bueno[1]

[1] *INRA, Neuro-Gastroenterology and Nutrition Unit, 31931 Toulouse, France*
[2] *Department of Pharmacology and Therapeutics, Faculty of Medicine, University of Calgary, Calgary, Alberta, Canada*
[3] *Department of Biological Sciences, University of Calgary, Calgary, Alberta, Canada*

Activation of colonic proteinase-activated receptor-2 (PAR_2) caused inflammation and increased mucosal permeability in mouse colon. The present study was aimed at characterizing the possible links between these two phenomena. We evaluated the effects of intracolonic infusion of PAR_2-activating peptide, SLIGRL, on colonic paracellular permeability and inflammation at two different doses, 5 and 100 μg per mouse, in an attempt to discriminate between both PAR_2-mediated effects. We further investigated the possible involvement of interferon γ (IFN-γ) and calmodulin-dependent activation of myosin light chain kinase (MLCK), and alterations of zonula occludens-1 (ZO-1) localization in PAR_2-induced responses. Thus, at the lower dose, SLIGRL increased colonic permeability without causing inflammation. Western blotting showed phosphorylation of mucosal myosin light chain (MLC) expression after both doses of SLIGRL. Moreover, while the MLCK inhibitor, ML-7, abolished the permeability effects of the low dose of SLIGRL, it only partially inhibited that of the high dose. In IFN-γ-deficient mice (B6 *ifng*$^{-/-}$), the increases in permeability were similar for both doses of SLIGRL and prevented by ML-7. In addition, MLCK immunoprecipitation revealed an increase of calmodulin binding to MLCK in the mucosa of mice treated with either dose of SLIGRL. Finally, we have shown that direct activation of PAR_2 on enterocytes is responsible for increased permeability and ZO-1 disruption. Moreover, SLIGRL at a dose that does not produce inflammation increases permeability via calmodulin activation, which binds and activates MLCK. The resulting tight junction opening does not depend upon IFN-γ secretion, while the increased permeability in response to the high dose of PAR_2 agonist involves IFN-γ secretion.

(Received 22 January 2004; accepted after revision 4 June 2004; first published online 11 June 2004)
Corresponding author L. Bueno: INRA, Neuro-Gastroenterology and Nutrition Unit,180 Chemin de Tournefeuille, BP.3, 31931 Toulouse cedex 9, France. Email: lbueno@toulouse.inra.fr

A major function of gastrointestinal epithelial cells is to form a physical barrier between the gastrointestinal lumen and subepithelial tissues. The apico-laterally located tight junctions (TJs) form a paracellular seal between the lateral membranes of adjacent cells. Lateral contacts, which may be visualized by electron microscopy and freeze-fracture analysis, act as a structural barrier against paracellular permeation (Jinguji & Ishikawa, 1992). Epithelial TJs are composed of at least three families of transmembrane proteins (occludins, claudins and adhesion proteins) and a cytoplasmic 'plaque' consisting of many different proteins that form large complexes. The transmembrane proteins mediate cell adhesion and are thought to constitute the intramembrane and paracellular diffusion barriers. The cytoplasmic plaque of TJs is formed by different types of proteins that include adaptors, such as the zonula occludens (ZO) proteins and other proteins that contain PDZ domains, as well as regulatory and signalling components. Adaptor proteins are thought to be connected to transmembrane proteins and to recruit other cytosolic components to TJs, such as protein kinases, GTPases and transcription factors (Mitic & Anderson, 1998). Several components of the cytoplasmic plaque, in addition to the transmembrane protein occludin, also function as cytoskeletal linkers that interact with the cytoskeleton (Mitic & Anderson, 1998). There is a high density of cytoskeletal actin and myosin filaments, which encircle the intestinal epithelial cells near the apical

 DOI: 10.1113/jphysiol.2004.061721

cellular borders at the level of TJs. The disruption of perijunctional actin–myosin filaments allows an increase in epithelial penetration (Yamaguchi *et al.* 1991). The activity of myosin is regulated by the opposing actions of myosin light-chain phosphatase and myosin light-chain kinase. Myosin light chain (MLC) phosphorylation by MLC kinase (MLCK) is one of the regulators of TJ permeability (Turner *et al.* 1997). In mice, stress-induced opening of colonic epithelial TJ requires $CD4^+/CD8^+$ T cells and IFN-γ, and involves MLCK activation (Ferrier *et al.* 2003). In the colon, a leaky TJ barrier allows penetration of toxic luminal substances, which promote colonic mucosal injury and inflammation (Gassler *et al.* 2001).

Proteinase-activated receptors (PARs) belong to a family of seven transmembrane domain G-protein-coupled receptors that are activated by cleavage of their N-terminal domain by a proteolytic enzyme (Nystedt *et al.* 1995). The unmasked new N-terminal sequence acts as a tethered ligand that binds and activates the receptor itself. PAR_2 is activated by trypsin, mast cell tryptase and trypsin-like proteins. Synthetic peptides, so-called PAR-activating peptides (PAR-APs) such as SLIGRL for PAR_2, corresponding to the amino-acid sequence of the tethered ligand, are also able to selectively activate PARs (Corvera *et al.* 1997). PAR_2 is found expressed throughout the gastrointestinal tract on several cell types, including enterocytes, mast cells, smooth muscle cells, myenteric neurones and endothelial cells (Kong *et al.* 1997). Moreover, the involvement of PAR_2 in different pathophysiological processes has been reported. In fact, *in vivo* intracolonic activation of PAR_2 led to colonic inflammation in mice and increased paracellular permeability, with bacterial translocation into peritoneal organs (Cenac *et al.* 2002). In this model, colonic infusion of trypsin, tryptase or SLIGRL induced a Th1-like inflammation, in which TNF-α, interleukin (IL)-1β and IFN-γ mRNA levels are elevated, while IL-4 and IL-10 mRNA expression remain stable (Cenac *et al.* 2002). *In vitro*, it has been shown that IFN-γ disrupts the epithelial barrier function of T84 cells by decreasing the levels of ZO-1, perturbing the actin cytoskeleton in the tight junction area, and displacing ZO-2 and occludin (Youakim & Ahdieh, 1999). In addition, TNF-α has been reported to promote the disturbing effects of IFN-γ on the epithelial barrier (Mahraoui *et al.* 1997), while IL-10 blocks these effects (Oshima *et al.* 2001). Although the expression of PAR_2 has been reported on both apical and basolateral surfaces of enterocytes, evidence is lacking so far that direct activation of PAR_2 may lead to a dysfunction of the epithelial barrier.

Consequently, the aim of this work was to determine the mechanisms underlying the effects of different concentrations of a PAR_2 agonist, the peptide SLIGRL, on colonic paracellular permeability. Specifically, we investigated (i) the involvement of IFN-γ, (ii) the involvement and activation pathway of MLCK, and (iii) the direct effects of PAR_2 agonist on enterocyte barrier functions.

Methods

Animals

This study was conducted on the one hand with Swiss 3T3 mice, since all our previous experiments use this strain (Cenac *et al.* 2002, 2003). On the other hand, to determine the role of IFN-γ we have used B6 *infg*$^{-/-}$ mice, which are IFN-γ deficient, and their control strain, C57BL/6J mice. Male Swiss 3T3 mice were from Janvier (Le Genest St-Isle, France) and B6 *ifng*$^{-/-}$ (IFN-γ deficient) and C57BL/6J (control strain of B6 *ifng*$^{-/-}$) mice were from The Jackson Laboratory (Bar Harbor, ME, USA). All mice were bred and maintained in the animal facility of the Institut Fédératif de Recherche Claude De Preval (INSERM IFR 30, Toulouse, France). Mice were housed in polycarbonate cages in a light- (12 h–12 h cycle) and temperature-controlled room (20–22°C) and were fed standard pellets (Safe A03; Epinay-sur-orge, France). Water was provided *ad libitum*. The experimental protocols described in this study were approved by the local Institutional Animal Care and Use Committee.

Intracolonic injections

Mice were fasted for 12 h before the beginning of experiments. Under deep xylazine–ketamine (5 : 1 ratio, 10 mg and 2 mg per mouse, respectively) anaesthesia, a small polyethylene catheter (0.3/0.07 mm) was inserted intrarectally at 4 cm from the anus. The PAR_2 activating peptide SLIGRL, the inactive reverse peptide LRGILS, or their vehicle (saline) was then injected into the colon through the catheter.

Experimental protocols

In previous experiments (Cenac *et al.* 2002), we demonstrated that peak inflammatory response to PAR_2 activation was observed at 4 h after intracolonic administration of the PAR_2 agonist (SLIGRL). Peak increase in paracellular permeability was observed from 2 to 4 h after SLIGRL administration. Thus, the 4-h time point was chosen for the present experiments. Four groups

of eight Swiss 3T3 mice received intracolonically (50 μl) SLIGRL (5 μg or 100 μg per mouse), LRGILS (100 μg per mouse) or saline (controls). Paracellular permeability, tissue inflammation, and Western-blot analysis of MLCK, MLC and p-MLC in colon, were assessed 4 h after intracolonic injections. Eight groups of eight B6 *ifng*$^{-/-}$ mice (deficient for functional IFN-γ) and eight groups of eight C57BL/6J mice (control strain for B6 *ifng*$^{-/-}$) received intracolonically saline, LRGILS (100 μg per mouse) or PAR$_2$-activating peptide (5 μg or 100 μg per mouse) as previously described. Four groups of IFNγ-deficient mice and four groups of wild-type mice were also treated with the MLCK inhibitor, ML-7 (2 mg kg−1, i.p.), while the remaining groups received the ML-7 vehicle. Here again, paracellular permeability, Western-blot for MLCK, MLC and p-MLC, and tissue inflammation were assessed 4-h after the intracolonic injections. Six groups of eight Swiss 3T3 mice received peptides as described earlier, and were pretreated with chlorpromazine (25 mg kg^{-1}, I.P.), a calmodulin inhibitor, or its vehicle, 30 min before peptide injection and paracellular permeability was assessed. Finally, MLCK immunoprecipitation was studied in four groups of eight Swiss mice that had received SLIGRL intracolonically.

Assessment of inflammation

At 4 h after intracolonic injection of SLIGRL, mice were killed by cervical dislocation and distal colon tissues collected. The severity of intestinal inflammation was evaluated by previously described criteria (Mombaerts *et al.* 1993) with slight modifications. Briefly, the disease score (0–10) was estimated by a combination of both gross and histological observations. The gross score (0–3) was rated:

(0) presence of normal beaded appearance;
(1) absence of beaded appearance of colon;
(2) focal thickened colon;
(3) marked thickness of the entire colon.

The histological score (0–7) was based upon the extent of:
intestinal wall thickening (0–3);
lamina propria infiltration (0–3);
presence (0–1) of ulceration.

In addition, colonic samples were assayed for myeloperoxidase (MPO) activity and RT-PCR (see below).

Myeloperoxidase activity assay

The activity of myeloperoxidase (MPO), which is found in polymorphonuclear neutrophil granules, was assessed in colon tissues according to the method of Bradley *et al.* (1982). Briefly, samples of distal colon (1 cm) were suspended in a potassium phosphate buffer (50 mM, pH 6.0) and homogenized in ice. Three cycles of freeze–thaw were undertaken. Suspensions were then centrifuged at 10 000 *g* for 15 min at 4°C. Supernatants were discarded and pellets were resuspended in hexadecyl trimethylammonium bromide buffer (HTAB 0.5% w/v, in 50 mM potassium phosphate buffer, pH 6.0). These suspensions were sonicated on ice, and centrifuged again at 10 000 *g* for 15 min at 4°C. The supernatants obtained were diluted in potassium phosphate buffer (pH 6.0) containing 0.167 mg ml^{-1} of *O*-dianisidine dihydrochloride and 0.0005% of hydrogen peroxide. Myeloperoxidase from human neutrophils (0.1 units per 100 μl) was used as a standard. The kinetic changes in absorbance at 450 nm, every 10 s over 2 min, were recorded with a spectrophotometer. One unit of MPO activity was defined as the quantity of MPO degrading 1 μmol of hydrogen peroxide min^{-1} ml^{-1} at 25°C. Protein concentration was determined with a commercial kit using a modified method of Lowry (Detergent Compatible Assay, Bio-Rad, Marnes la Coquette, France). MPO activity was expressed as units per gram of protein.

RT-PCR detection of β-actin, IL-10, IFN-γ and TNF-α mRNA

For RT-PCR detection of cytokine RNA, total RNA (5–10 μg) was reverse-transcribed into complementary DNA (cDNA) using Superscript II RNase H$^-$ RT (Gibco-BRL, Cergy Pontoise, France). The primers used were: β-actin: 5′-GGG TCA GAA GGA TTC CTA TG-3′ and 5′-GGT CTC AAA CAT GAT CTG GG-3′; IL-10: 5′-ATG CAG GAC TTT AAG GGT TACT TG-3′ and 5′-AGA CAG CTT GGT CTT GGA GCT TA-3′; IFN-γ: 5′-GCT CTG AGA CAA TGA ACG CT-3′ and 5′-AAA GAG ATA ATC TGG CTC TGC-3′; TNF-α: 5′-TCT CAT CAG TTC TAT GGC CC-3′ and 5′-GGG AGT AGA CAA GGT ACA AC-3′. Competitive PCR analysis was performed using linearized plasmids: pQB3 for the competition with β-actin, and pMus3 for the competition with IFN-γ, IL-10 and TNF-α (Legoux *et al.* 1992; Zou *et al.* 1995). Amplification was performed for 40 cycles consisting of denaturation for 1 min at 94°C, primer annealing for 1 min at 52–55°C, and primer extension for 1.5 min at 72°C. DNA products were then separated on a 3% agarose gel with ethidium bromide and the ratio between amplified molecules for the target cDNA and the competitor, i.e. log (DNA competitor/target cDNA), was calculated for each graded concentration of the competitor, using an image

analyser (QuantityOne software; Amersham Pharmacia, Orsay, France). A curve of the ratios was established according to the competitor concentrations. This allowed the calculation of the equivalence point, at which the amount of amplified target mRNA and DNA competitor are equal (log (DNA competitor/target cDNA) = 0). This value corresponds to the concentration of the target cDNA present in the initial sample (Legoux *et al.* 1992; Zou *et al.* 1995). To quantify cytokines in samples more accurately, the number of cytokine molecules was expressed in comparisson with the number of cDNA molecules of the internal control, β-actin, in the same sample.

In vivo permeability studies

Mice were anaesthetized with xylazine–ketamine (5 : 1 ratio, 10 mg and 2 mg per mouse, respectively; subcutaneously). To measure colonic paracellular permeability, 0.7 μCi of ^{51}Cr-EDTA (Perkin Elmer Life Sciences, Paris, France) in 0.5 ml NaCl (154 mM) was slowly infused into the colon (0.25 ml h^{-1}). After 2 h, mice were killed by cervical dislocation and colons were removed. Then, colons and remaining bodies were placed in separate counting tubes in a gamma-counter (Packard Cobra II, Packard Bioscience, Meriden CT, USA). The permeability was expressed as the ratio between body and total (body plus colon) radioactivities.

In vitro cell culture

SCBN cells are human non-transformed enterocytes, which form polarized monolayers with functional tight junctions and contain cytokeratins, mucin antigen, and messenger RNA for epidermal growth factor, IL-6, and vascular adhesion molecule-1 (Pang *et al.* 1996). Cells from passages 22–26 were grown to confluence in Dulbecco's modified Eagle's medium (DMEM, Sigma, St Louis, MO, USA) supplemented with 5% or 10% fetal bovine serum (Sigma), 100 μg ml^{-1} streptomycin, 100 U ml^{-1} penicillin, 0.08 mg ml^{-1} tylosine and 200 mmol L-glutamine (all from Sigma) and incubated at 37°C, 5% CO_2 and 96% humidity in chamber slides or Transwells (Costar, Corning, NY, USA).

In vitro permeability measurements

Permeability studies were performed *in vitro* to further investigate altered barrier function in response to PAR_2-AP. SCBN monolayers were grown to confluence on Transwell membranes in 12-well plates (Costar). Five-day-old confluent monolayers develop electrical resistances of $> 1200\ \Omega\ cm^{-2}$ as measured with an electrovoltohmeter (EVOM; World Precision Instruments, Sarasota, FL, USA). Permeability was assessed by measuring apical to basolateral fluxes of fluorescein isothiocyanate (FITC)–dextran (relative molecular mass 3000, 100 μmol l^{-1}; Molecular Probes, Eugene, OR, USA) across the monolayers. Confluent SCBN monolayers on Transwell membranes were washed 3 times in sterile tissue culture-grade PBS (Sigma) to remove residual media. The upper chambers of the Transwells were filled with 300 μl of Krebs buffer. The following treatments were added to either the upper or the lower chamber: Vehicle control (DMEM), LRGILS 25 μM or SLIGRL (25 μM). Then the monolayers were incubated for 2 h in the dark at 37°C, 5% CO_2 and 96% humidity. After this incubation, two 300-μl samples were removed from the bottom chamber, and fluorescence was measured on a microplate fluorometer (SpectraMax Gemini; Molecular Devices, Sunnyvale, CA, USA) along with samples of the original apical solution. The FITC–dextran flux was measured as the percentage of the original apical solution that can be detected in the basolateral medium that crossed 1 cm^2 in 1 h, as previously described (Chin *et al.* 2002; Scott *et al.* 2002).

Immunoprecipitation of MLCK

To investigate the interaction between MLCK and calmodulin, MLCK was immunoprecipited and Western blot analyses of MLCK and calmodulin were performed. For immunoprecipitation, colonic mucosal tissues were scraped into 500 μl of 1% Triton X-100 lysis buffer (50 mM Hepes, 150 mM NaCl, 1% Triton X-100, protease inhibitor cocktail (Sigma, Saint-Quentin Fallavier, France)) and clarified by centrifugation at 4°C for 15 min at 14 0000 *g*. Before the immunoprecipitation, anti-MLCK IgG (Santa Cruz Biotechnology, Inc., Santa Cruz, CA, USA) was bound to protein G–Sepharose (Sigma) in HNT buffer (30 mM Hepes, 30 mM NaCl, 0.1% Triton X-100; pH 7.5). The supernatant was incubated with the antibody–protein G–Sepharose (Sigma) for 7 h at 4°C. Immune complexes were collected by centrifugation, washed 3 times in buffer (30 mM Hepes, 30 mM NaCl, 0.1% Triton X-100; pH 7.5), and treated for Western blot analysis.

Western blot analysis for calmodulin, MLCK, MLC and p-MLC

Mice were killed by cervical dislocation. After laparotomy, colons were collected and washed with saline, and the mucosa was scraped off and recovered. Proteins

were extracted with Tri-reagent (Gibco-BRL, Eragny, France) and solubilized with 1% SDS (Sigma). Protein concentration was assessed using the DC protein assay kit (Bio-Rad, France). Equal amounts of each extract were then subjected to SDS-PAGE in 12% (MLC and phospho-MLC determination) or 7.5% (MLCK) slabs, then electro-transferred onto 0.45 mm nitrocellulose membrane. Membrane was blocked with Tris-buffered saline (TBS)–milk 6%, then incubated overnight at 4°C with the primary antibody. We used a 1/1000 dilution for all primary antibodies, i.e. anti-MLC, anti-phospho-MLC, anti-CaM (Santa Cruz Biotechnology), and anti-MLCK (Sigma). Sodium fluoride (10 mM) was added for phospho-MLC determination. After washing, peroxidase-labelled G-protein (Sigma) was added for 1 h at room temperature. The membrane was incubated for 1–5 min with SuperSignal Reagent (Pierce, Bezons, France).

Electron microscopy of tight junction

Three Swiss 3T3 mice per group (treated and controls) were killed 4 h after SLIGRL (5 μg per mouse), LRGILS (100 μg per mouse) or saline infusion. Colons were removed and cut into 2 mm pieces. Tissue samples were fixed in 2.5% glutaraldehyde–2% paraformaldehyde solution (1 h; +4°C), rinsed in 0.1 M cacodylate buffer and post-fixed for 1 h at +4°C in 1% osmium tetroxide. Subsequently, tissue samples were dehydrated by graded ethanol and embedded in Epon-Araldite resin (Euromedex, Mundolsheim, France). Ultra-thin sections (70 nm) were carried out with an ultramicrotome system (Reichert, Leica, Rueil-Malmaison, France) and collected on copper–palladium grids. After staining with 4% uranyl acetate and 0.4% lead citrate, sections were examined with a Hitachi HU11C electron microscope (Hitachi, Paris, France).

Immunohistochemistry for ZO-1

SCBN monolayers were incubated with 400 μl of SLIGRL (30 μM), LRGILS (30 μM) or DMEM (vehicle control) for 2 h. After permeabilization, monolayers were washed 3 times for 10 min each time in sterile PBS (Sigma) and blocked with fetal bovine serum (FBS, Sigma) for 10 min at room temperature. After three more 10-min washes with sterile PBS, monolayers were incubated with an affinity-purified polyclonal rabbit anti-human ZO-1 antibody (Santa Cruz Biotechnology), 100 μl diluted 1 : 100 in PBS, or 100 μl of Cy3-conjugated sheep anti-rabbit IgG (1 : 100 in PBS) for 60 min at room temperature. Slides were washed 3 times for 10 min each time in sterile PBS, and 200 μl of Cy3-conjugated sheep anti-rabbit IgG (1 : 100 in PBS) was added to each well. After a 60-min incubation in a humidity chamber at room temperature, slides underwent three more 10-min washings in PBS and then were mounted with Aqua Poly Mount (Poly Sciences) and examined on a confocal laser scanning microscope (ViewScan DVD-250; Bio-Rad, Hercules, CA, USA). Micrographs were obtained with a Spot II digital camera (Diagnostic Instruments, Sterling Heights, MI, USA).

Chemicals

Peptides, SLIGRL-NH_2 and LRGILS-NH_2 (referred to in the text as SLIGRL and LRGILS), prepared by solid phase synthesis, were obtained from Neosystem (Strasbourg, France). The composition and purity of peptides were confirmed by HPLC analysis. SLIGRL and LRGILS were dissolved in saline. The MLCK inhibitor, 1-(5-iodonaphtalene-1-sulphonyl)-1H-hexahydro-1,4-diazepine (ML-7), and the calmodulin inhibitor, chlorpromazine were obtained from Sigma (France). ML-7 was dissolved in 2% ethanol and 98% saline; chlorpromazine was dissolved in saline.

Statistical analysis

Data are presented as means ± standard error of the mean. Analyses were done by running the GraphPad Prism 3.0 software (GraphPad, San Diego, CA, USA). All data were normally distributed. Between-group comparisons were performed by Student's unpaired *t* test. Multiple comparisons within groups were performed by repeated-measures one-way ANOVA, followed by Student's *t* test. Statistical significance was accepted at $P < 0.05$.

Results

A low dose of PAR_2-AP increases colonic paracellular permeability without causing inflammation

As we have previously shown in Swiss 3T3 mice that PAR_2 agonists administered intracolonically caused colon inflammation and increased paracellular permeability, we used the same strain of mice to further study the relationship between inflammation and permeability for different doses of the PAR_2 agonist. In colons of Swiss 3T3 mice, the intracolonic administration of SLIGRL (100 μg per mouse, considered as a high dose of PAR_2 activating peptide) caused significant increase

Table 1. Inflammatory parameters in Swiss mice after intracolonic administration of SLIGRL (5 or 100 μg per mouse), LRGILS (100 μg per mouse) or saline

	Saline	100 μg LRGILS	5 μg SLIGRL	100 μg SLIGRL
MPO (U (g of protein)$^{-1}$)	84 ± 8	49 ± 5	78 ± 10	638 ± 198*
Damage score	0.5 ± 0.11	0.8 ± 0.06	1.1 ± 0.12	5.8 ± 0.60*
TNF-α	2.36 ± 0.23	2.10 ± 0.15	2.23 ± 0.38	4.39 ± 0.51*
IFN-γ	0.11 ± 0.01	0.18 ± 0.04	0.13 ± 0.02	0.70 ± 0.03*
IL-10	1.46 ± 0.12	1.16 ± 0.09	1.28 ± 0.21	0.47 ± 0.11*
Permeability (%)	1.8 ± 0.4	1.4 ± 0.2	3.3 ± 0.2*	6.6 ± 0.6*

*$P < 0.05$ compared with 'saline' values. The number of cytokine molecules was expressed in comparison with the number of cDNA molecules of the internal control, β-actin, in the same sample. Permeability was expressed in a percentage of ^{51}Cr-EDTA permeability.

in MPO activity, damage score, TNF-α and IFN-γ mRNA expressions, caused increased paracellular permeability, and a significant decrease in IL-10 mRNA expression (Table 1). In contrast, a markedly lower dose of SLIGRL (5 μg per mouse) increased paracellular permeability ($3.3 \pm 0.2\%$ *versus* $1.4 \pm 0.2\%$; $P < 0.05$) without concurrent inflammatory reaction: MPO activity, damage score and TNF-α, IFN-γ and IL-10 expression being equivalent to those observed in controls (Table 1). The reverse peptide LRGILS, inactive on PAR_2 (100 μg per mouse), had no effect on both inflammatory parameters and paracellular permeability (Table 1). The increase of paracellular permeability mediated by the high dose of SLIGRL was significantly greater than that obtained with the low dose (Table 1). Both doses of SLIGRL increased MLC phosphorylation, without affecting quantities of MLCK and MLC (Fig. 1*A*). Furthermore, tight junction opening after the low dose of SLIGRL was clearly observed by electron microscopy of colonic epithelial cells (Fig. 1*B*). The reverse peptide LRGILS had no effect on the expression of MLCK, MLC and p-MLC (Fig. 1*A*).

The inflammatory reaction mediated by PAR_2 activation in wild-type mice is abolished in IFN-γ-deficient mice

To investigate the involvement of IFN-γ in PAR_2-induced colitis and increased permeability, we used IFN-γ-deficient mice, which are available only in a C57BL/6J background. Therefore, we reproduced in C57BL/6J mice the experiments previously performed in Swiss 3T3. In C57BL/6J, the intracolonic administration of SLIGRL (100 μg per mouse) also caused a significant increase in MPO activity, damage score and TNF-α mRNA expression, and a significant decrease in IL-10 mRNA expression (Table 2). The reverse peptide LRGILS had no effect on the inflammatory parameters measured (Table 2). In contrast, low doses of SLIGRL (5 μg per mouse) caused no inflammation: MPO activity, damage score and TNF-α and IL-10 expression were similar to those in saline-treated mice (Table 2). Furthermore, in IFN-γ-deficient mice, administration of either SLIGRL (5 and 100 μg per mouse) or the reverse peptide LRGILS (100 μg per mouse) had no effect on the different inflammatory parameters measured (Table 3).

PAR_2 activation increases permeability in wild type and IFN-γ-deficient mice by MLCK activation

In wild-type mice (C57BL/6J) as well as in Swiss 3T3 mice, the increase of colonic paracellular permeability mediated by the high dose of SLIGRL (100 μg per mouse) was significantly higher than that mediated by the low dose (5 μg per mouse) (Fig. 2*A*). In contrast, in IFN-γ-deficient mice (B6 *ifng*$^{-/-}$), the increased paracellular permeability mediated by SLIGRL was not significantly different for the two doses of SLIGRL ($3.3 \pm 0.2\%$ *versus* $3.5 \pm 0.2\%$ for 5 and 100 μg per mouse, respectively; $P = 0.6$), but was significantly higher compared to saline-injected mice (Fig. 2*A*). The reverse peptide LRGILS had no effect on paracellular permeability in both wild-type and IFN-γ-deficient mice (Fig. 2*A*). Pretreatment of C57BL/6J by the MLCK inhibitor, ML-7, diminished the increased paracellular permeability mediated by the high dose of SLIGRL ($4.0 \pm 0.6\%$ *versus* $5.8 \pm 0.5\%$; $P < 0.05$) and abolished the effect mediated by the low dose ($1.2 \pm 0.2\%$ *versus* $3.1 \pm 0.5\%$; $P < 0.05$) (Fig. 2*A*). In contrast, in the IFN-γ-deficient mice, ML-7 prevented the increase of paracellular permeability for both doses of SLIGRL (high dose: $1.7 \pm 0.3\%$ *versus* $3.5 \pm 0.2\%$, $P < 0.05$; low dose: $1.4 \pm 0.2\%$ *versus* $3.3 \pm 0.2\%$, $P < 0.05$) (Fig. 2*A*).

PAR_2 activation increases MLC phosphorylation in wild-type and IFN-γ-deficient mice by MLCK activation

In IFN-γ-deficient mice (B6 *ifng*$^{-/-}$) and in wild-type mice (C57BL/6J), both doses of SLIGRL induced similar

increases of MLC phosphorylation (Fig. 2*B*) and had no effect on the quantity of MLC and MLCK (Fig. 2*B*). ML-7 (2 mg kg^{-1}) inhibited MLC phosphorylation in the two strains of mice and had no effect on MLC and MLCK expression (Fig. 2*B*).

PAR$_2$-induced activation of MLCK is calmodulin dependent

In Swiss 3T3 mice, inhibition of calmodulin by chlorpromazine (25 mg kg^{-1}), diminished the increase of paracellular permeability induced by the high dose (100 μg per mouse) of SLIGRL ($3.9 \pm 0.4\%$ *versus* $6.8 \pm 0.4\%$; $P < 0.05$) and abolished that induced by the low dose (5 μg per mouse) of SLIGRL ($1.9 \pm 0.2\%$ *versus* $3.5 \pm 0.3\%$; $P < 0.05$) (Fig. 3*A*). Chlorpromazine had no effect *per se* on paracellular permeability. MLCK immunoprecipitation revealed an increase of calmodulin bound to MLCK in SLIGRL-treated mice compared to those treated with saline or the reverse peptide LRGILS (Fig. 3*B*).

In vitro, basal but not apical activation of PAR$_2$ increases epithelial permeability

Apical to basolateral fluxes of FITC–dextran 3000 were measured to assess whether apical or basal exposure of SCBN monolayers to SLIGRL (30 μM) for 2 h could reproduce the PAR$_2$-AP-induced loss of intestinal barrier function observed in mice *in vivo*. Apical exposure of SLIGRL had no effect on transepithelial dextran fluxes (Fig. 4). In contrast, basal exposure of SCBN monolayers to SLIGRL significantly increased dextran fluxes (0.37 ± 0.02 *versus* $0.23 \pm 0.01\%$ apical FITC–dextran cm^{-2} h^{-1}; $P < 0.05$). Neither apical nor basal exposure

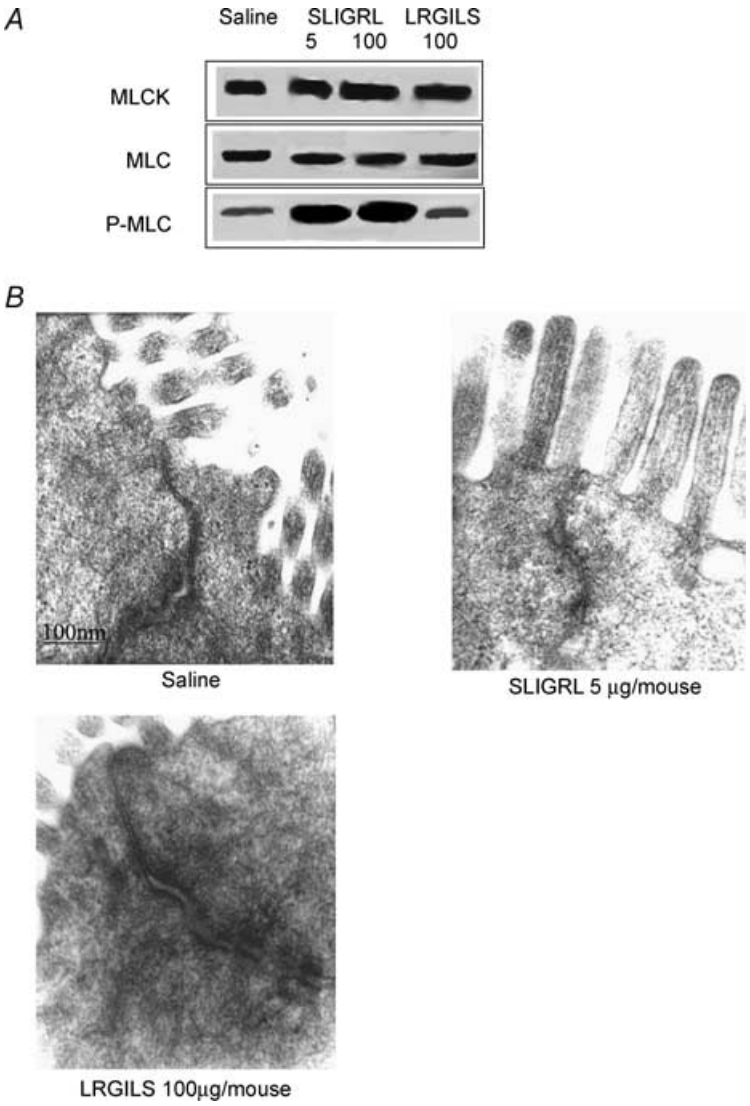

Figure 1. MLCK, MLC and p-MLC and electron microscopy of tight junctions
A, detection of MLCK, MLC and p-MLC proteins by Western blot. Mice (Swiss 3T3) received intracolonocally SLIGRL (5 and 100 μg per mouse), LRGILS (100 μg per mouse) or their vehicle (saline). Mucosa lysates were incubated with anti-mouse MLCK, MLC or p-MLC antibodies. MLCK, MLC and p-MLC were detected as bands with a molecular mass of about 130, 20 and 20 kDa, respectively ($n = 5$). *B*, electron microscopy of tight junction observed in mice Swiss 3T3 colon treated with SLIGRL (5 μg per mouse), LRGILS (100 μg per mouse) or saline ($n = 3$).

Table 2. Inflammatory parameters in C57BL/6 J mice (control strain of B6 *ifng*$^{-/-}$ mice) after intracolonic administration of SLIGRL (5 or 100 μg per mouse), LRGILS (100 μg per mouse) or saline

	Saline	100 μg LRGILS	5 μg SLIGRL	100 μg SLIGRL
MPO (U (g of protein)$^{-1}$)	99 ± 21	96 ± 9	101 ± 13	759 ± 71*
Damage score	0.9 ± 0.05	1.1 ± 0.03	1.5 ± 0.08	6.3 ± 0.82*
TNF-α	2.18 ± 0.21	2.21 ± 0.19	1.95 ± 0.41	5.04 ± 0.81*
IL-10	1.08 ± 0.07	0.91 ± 0.08	1.21 ± 0.06	0.36 ± 0.13*

*$P < 0.05$ compared with 'saline' values. (see Table 1 for legend).

Table 3. Inflammatory parameters in B6 *ifng*$^{-/-}$ (IFNγ-deficient) mice after intracolonic administration of SLIGRL (5 or 100 μg per mouse), LRGILS (100 μg per mouse) or saline

	Saline	100 μg LRGILS	5 μg SLIGRL	100 μg SLIGRL
MPO (U (g of protein)$^{-1}$)	92 ± 23	92 ± 11	81 ± 21	76 ± 15
Damage score	0.8 ± 0.06	0.6 ± 0.14	0.7 ± 0.08	1.1 ± 0.12
TNF-α	1.22 ± 0.18	1.32 ± 0.09	1.45 ± 0.15	1.68 ± 0.13
IL-10	0.9 ± 0.04	0.9 ± 0.08	1.2 ± 0.12	1.08 ± 0.10

*$P < 0.05$ compared with 'saline' values. (see Table 1 for legend).

of SCBN monolayers to the reverse peptide LRGILS had any effect on transepithelial dextran fluxes.

PAR_2 activation induces reorganization of epithelial ZO-1

In control SCBN monolayers, tight junctional ZO-1 was characteristically located at the cellular margins (Fig. 5*A*). After a 2-h incubation with SLIGRL (30 μM), ZO-1 migrated from the cellular margins into the cytoplasm (Fig. 5*B*). The reverse peptide LRGILS (30 μM) did not change tight junctional ZO-1 localization (Fig. 5*C*).

Discussion

Our study reveals for the first time that (i) a low dose of SLIGRL increases paracellular permeability via MLC phosphorylation by MLCK without causing inflammation, and (ii) that the increase in paracellular permeability mediated by the inflammatory dose of SLIGRL involves an INF-γ-dependent mechanism. Activation of PAR_2 by low doses of SLIGRL provoked the activation of calmodulin, which interacts with and stimulates MLCK most likely in epithelial cells, without concomitant influence of inflammatory factors. In fact, for all strains of mice studied here, low doses of PAR_2-AP had no effect on inflammatory parameters. By electron microscopy, we have shown that a low dose of SLIGRL opened epithelial cell tight-junctions with a concurrent activation of MLCK, which in turn, led to an increase in p-MLC proteins observed by Western-blot analysis. Moreover, PAR_2 agonist relocalized ZO-1 and increased paracellular permeability in epithelial monolayers, further demonstrating a direct effect of PAR_2 activation on enterocytes. In C57BL/6J and Swiss 3T3 mice, permeability was dose-dependently increased after SLIGRL. While ML-7 abolished the effect of the low dose of SLIGRL, it only decreased that of the high dose. In these mice, high doses of SLIGRL provoked an inflammatory reaction characterized by increased MPO activity, high damage scores, increased IFN-γ and TNF-α mRNA, and decreased IL-10 mRNA. In IFN-γ-deficient mice, SLIGRL had no effect on inflammatory parameters, but increased intestinal permeability to the same extent for both doses of SLIGRL. This increase in paracellular permeability was linked to MLCK activation. The inflammatory reaction is IFN-γ dependent and for the high dose of SLIGRL the paracellular permeability is IFN-γ and calmodulin–MLCK dependent. In contrast, for the low dose of SLIGRL, the increase in paracellular permeability depends on calmodulin–MLCK activation, but not on IFN-γ.

In previous studies, we have shown that the inflammatory reaction mediated by high doses of SLIGRL was inhibited by chronic pretreatment with either capsaicin, or by NK1 or CGRP receptor antagonist suggesting a neurogenic component of this inflammation (Cenac *et al.* 2003; Nguyen *et al.* 2003). While the inflammatory response was inhibited by such treatments, a residual increase of paracellular permeability was still observed and was of the same magnitude as the increase observed for a low dose of SLIGRL (Cenac *et al.* 2003). The calmodulin–MLCK complex, as well as inflammatory

mediators such as IFN-γ are involved in SLIGRL-induced paracellular permeability increase during inflammation. Indeed, in B6 *ifng*$^{-/-}$ mice, the increase in permeability was similar for both doses of SLIGRL and prevented by ML-7. The high dose of SLIGRL did not increase MPO activity, damage score, or TNF-α and IL-10 mRNA in these IFN-γ-deficient mice.

The increased permeability response to PAR_2 activation may not be linked to selective activation of PAR_2 located at the apical site of epithelial cell membrane as *in vitro*, only when PAR_2 agonist was added to the basolateral side of SCBN monolayers, permeability to FITC–dextran was increased. However, it is not known whether PAR_2 presents the same distribution on apical and basal sides of

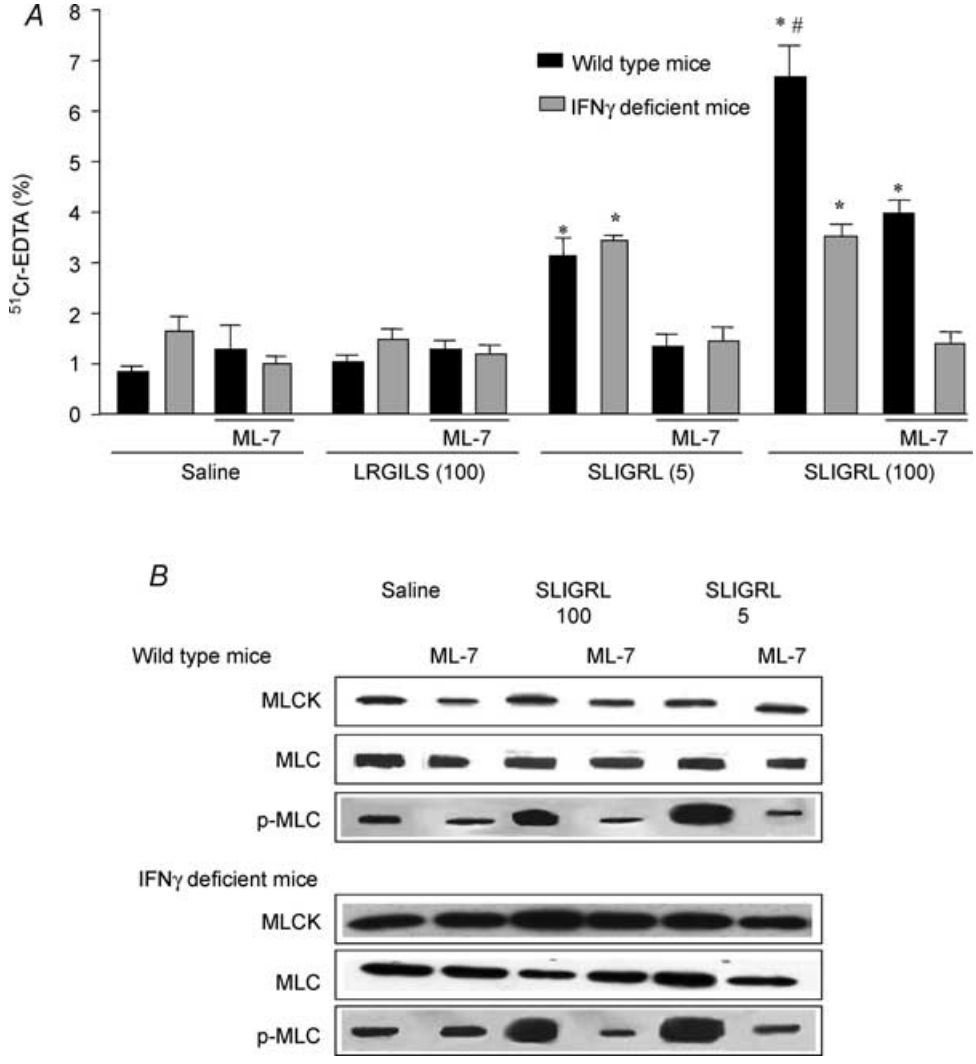

Figure 2. Prevention by MLCK inhibitor of SLIGRL-induced intracellular permeability increase and MLC phosphorylation

A, prevention by the MLCK inhibitor, ML-7, of SLIGRL-induced colonic paracellular permeability increase. B6 *ifng*$^{-/-}$ mice (IFN-γ deficient) and their control strain (C57BL/6J) were pretreated by ML-7 (2 mg kg^{-1}) and received intracolonic administration of saline, LRGILS (100 μg per mouse) or SLIGRL (5 and 100 μg per mouse). Intestinal permeability was assessed by measuring the gut lumen-to-body passage of labelled ^{51}Cr-EDTA. Values are means ± S.E.M.; $n = 8$; $^*P < 0.05$ compared to 'saline' values, $\#P < 0.05$ compared to the values of the group treated by 5 μg per mouse of SLIGRL. *B*, detection of MLCK, MLC and p-MLC proteins by Western blot. IFN-γ-deficient and wild-type mice were treated by SLIGRL (5 and 100 μg per mouse) or its vehicle (saline) and pretreated by a MLCK inhibitor, ML-7 (2 mg kg^{-1}, i.p.), or its vehicle (2% ethanol). Mucosa lysates were incubated with anti-mouse MLCK, MLC or p-MLC antibodies. MLCK, MLC and p-MLC were detected as bands with a molecular mass of about 130, 20 and 20 kDa, respectively ($n = 5$).

epithelial cell membranes *in vitro* and *in vivo*. We hypothesize that the non-inflammatory permeability response to PAR_2 activation is linked to the activation of a subset of receptors, with distinct intracellular pathways. Indeed, in human airway smooth muscle cells, PAR_2 activation stimulates phospholipase C (PLC) via its coupled Gq protein (Berger *et al.* 2001). The activation of the PLC-dependent signalling pathway has been implicated in the assembly, regulation and barrier properties of the tight junction (Balda *et al.* 1991). In fact activation of PLC releases IP_3 into the cytosol, which increases intracellular Ca^{2+} concentration, which activates MLCK through the activation of calmodulin-dependent kinases (Berridge *et al.* 1983; Streb *et al.* 1983). MLCK phosphorylates MLC and thereby induces contraction of the perijunctional actin–myosin ring, which has been reported to provoke the opening of tight junctions (Yamaguchi *et al.* 1991). The increase in paracellular permeability caused by ethanol (Ma *et al.* 1999) and medium chain fatty acids, such as capric and lauric acid (Lindmark *et al.* 1998), as well as that caused by microbes (Scott *et al.* 2002) are attributed to this mechanism. Ethanol caused disassembly and displacement of perijunctional actin–myosin ring and stimulates MLCK (Ma *et al.* 1999). The inhibitor of MLCK (ML-7) attenuated both the ethanol-mediated increase in paracellular permeability and MLCK activity (Ma *et al.* 1999). Similarly, chelation of cytosolic Ca^{2+} and inhibition of MLCK attenuated the ability of capric and lauric acid to increase paracellular permeability (Lindmark *et al.* 1998). In our study we show that the activation of PAR_2 increases the interaction of calmodulin and MLCK probably by an increase of intracellular Ca^{2+} concentration. This hypothesis is further supported by the fact that in many cell types, PAR_2 activation causes intracellular calcium mobilization. This complex favours MLC phosphorylation and perijunctional actin–myosin ring contraction leading to alteration of paracellular permeability.

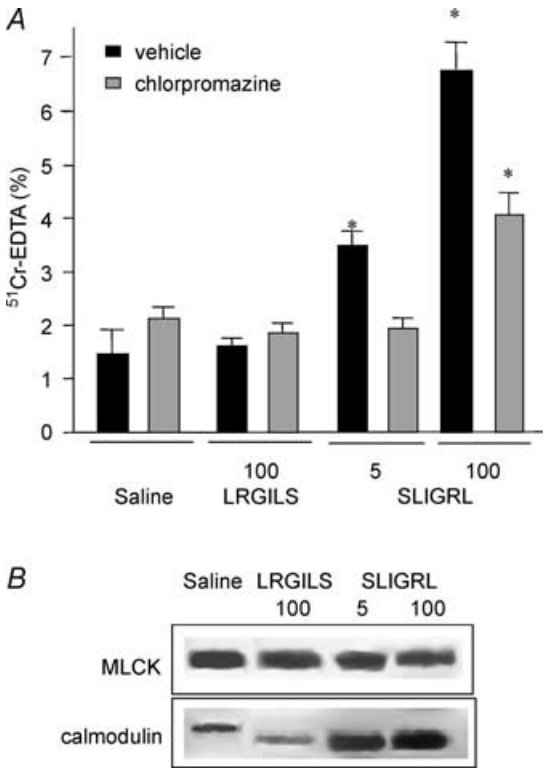

Figure 3. Interaction between MLCK and calmodulin
A, inhibition by the calmodulin inhibitor, chlorpromazine, of SLIGRL-induced colonic paracellular permeability increase. Swiss 3T3 mice were pretreated by chlorpromazine (25 mg kg^{-1}, I.P.) (grey bars) or its vehicle (saline) (black bars) and received intracolonically saline, LRGILS (100 μg per mouse) or SLIGRL (5 and 100 μg per mouse). Intestinal permeability was assessed by measuring the gut lumen-to-body passage of labelled ^{51}Cr-EDTA. Values are means ± S.E.M.; $n = 8$; $^*P < 0.05$ compared to 'saline' values. *B*, calmodulin–MLCK interactions. Four hours after treatment of Swiss 3T3 mice by saline, LRGILS (100 μg per mouse) or SLIGRL (5 and 100 μg per mouse), colons were removed, and colonic mucosa proteins were immunoprecipitated with an anti-MLCK antibody followed by calmodulin and MLCK immunoblotting assays. MLCK and calmodulin were detected as bands with a molecular mass of about 130 kDa and 16 kDa, respectively ($n = 5$).

At a higher dose, PAR_2-AP may be absorbed, and subsequently activates receptors located at the baso-lateral site of epithelial cells or other cell types such as immunocytes or nerves, inducing a neurogenic inflammation (Cenac *et al.* 2003; Nguyen *et al.* 2003). In agreement with this hypothesis, capsaicin inhibits the inflammatory reaction and diminishes the increase in permeability (Cenac *et al.* 2003). Results obtained in IFN-γ-deficient mice confirmed the crucial role of IFN-γ since no inflammation was seen even with a high dose of PAR_2-AP in these animals. Disruption of the epithelial barrier in the gut is a hallmark of inflammatory bowel disease (IBD) and intestinal infections (Gitter *et al.* 2001). Although it remains unclear whether barrier breakdown is an initiating event or a consequence of inflammation, it is obvious that barrier loss contributes to propagation and exacerbation of inflammation (Gassler *et al.* 2001). Barrier breakdown can be elicited by a number of agents, including bacteria, immunocytes, and proinflammatory cytokines. Previous studies have demonstrated that T84 cells exposed to IFN-γ show decreased barrier function integrity (Youakim & Ahdieh, 1999). IFN-γ is greatly elevated in human intestinal disease and undoubtedly contributes to the inflammatory cascade, which includes barrier disruption. In fact, IFN-γ acts on at least two elements critical to barrier function. The first is to cause a decrease in the expression of ZO-1, a key component

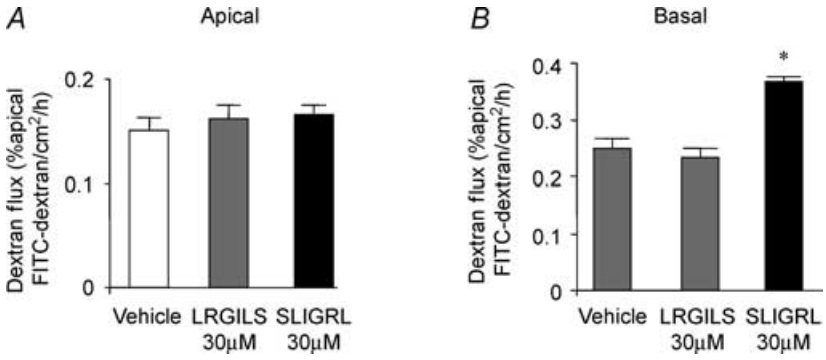

Figure 4. Paracellular permeability of SCBN monolayers, measured as transepithelial flux of FITC-dextran 3000
Values were obtained from control monolayers with vehicle and monolayers incubated with SLIGRL (30 μM) or LRGILS (30 μM) for 2 h (apical, *A*, and basal, *B*). Values are means ± S.E.M. of the percentage apical fluorescence that crossed 1 cm^2 of the epithelial barrier into the basolateral chamber in 1 h. $^*P < 0.05$ compared to saline values; $n = 12$ per group.

of the tight junction (Youakim & Ahdieh, 1999). The second is to alter the organization of the actin cytoskeleton in the apical region of the cells (Youakim & Ahdieh, 1999). TNF-α can enhance these effects, probably due to IFN-γ-dependent increase in TNF receptor gene expression suggesting that, in IBD, TNF-α may have synergistic effects on IFN-γ-mediated alterations of epithelial cell function (Rodriguez *et al.* 1995). In a recent study carried out on 23 patients with active Crohn's disease, it was demonstrated that treatment with TNF antibodies largely restores the gut barrier (Suenaert *et al.* 2002). Recent clinical trials provided evidence for a therapeutic effect of IL-10 in patients with Crohn's disease by reducing intestinal inflammation (Schmit *et al.* 2002). One potential explanation for the observed inhibition of IFN-γ effects on barrier function by IL-10 could be that IL-10 down-regulates receptors for IFN-γ (Oshima *et al.* 2001). A beneficial effect of IL-10 is its ability to block the reduced expression of occludin induced by IFN-γ (Oshima *et al.* 2001).

PAR_2 activation at an 'inflammatory dose' of SLIGRL was associated with an increase in TNF-α, IFN-γ and IL-1β expression and a decrease in IL-10 expression. Thus, we can hypothesize that the Th1 profile mediated

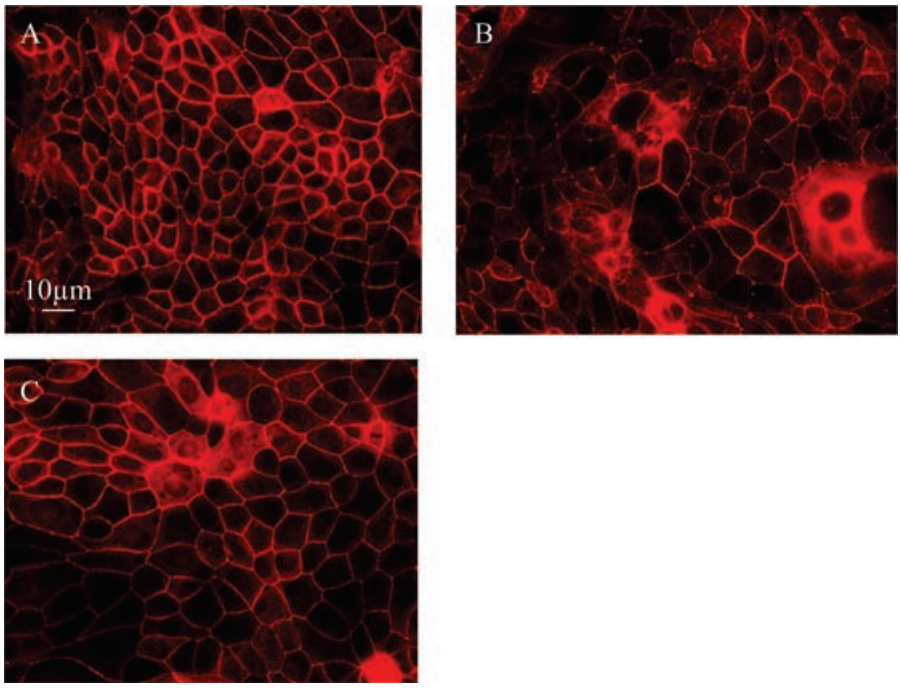

Figure 5. Representative confocal laser scanning micrographs of SCBN monolayers stained for tight junctional ZO-1
A, preparations included unmanipulated control monolayers: typical distribution of ZO-1 in control monolayers can be seen at the periphery of the enterocytes; *B*, monolayers exposed to SLIGRL (30 μM) for 2 h: exposure to SLIGRL causes a perinuclear relocation of ZO-1; *C*, monolayers exposed to LRGILS (30 μM) for 2 h: LRGILS had no effect.

by PAR_2 activation during the inflammatory reaction increased paracellular permeability by a combined action of IFN-γ and TNF-α on the expression of ZO-1 and on the organization of the actin cytoskeleton in the apical region. This hypothesis is supported by the reduction of paracellular permeability increase in mice deficient for IFN-γ.

In summary, in non-inflammatory conditions, PAR_2 activation increases paracellular permeability through calmodulin activation, which can bind to and activate MLCK, and then provokes tight junction opening by peri-junctional ring myosin phosphorylation. In inflammatory conditions increased paracellular permeability is mediated by the pathway described above and by an IFNγ-dependent pathway.

Acknowledgements

The authors thank B. Joseph for his technical assistance and Institut National de la Recherche Agronomique for its financial support.

References

Balda MS, Gonzalez-Mariscal L, Contreras RG, Macias-Silva M, Torres-Marquez ME, Garcia-Sainz JA & Cereijido M (1991). Assembly and sealing of tight junctions: possible participation of G-proteins, phospholipase C, protein kinase C and calmodulin. *J Membr Biol* **122**, 193–202.

Berger P, Tunon-De-Lara JM, Savineau JP & Marthan R (2001). Selected contribution: tryptase-induced PAR-2-mediated Ca^{2+} signaling in human airway smooth muscle cells. *J Appl Physiol* **91**, 995–1003.

Berridge MJ, Dawson RM, Downes CP, Heslop JP & Irvine RF (1983). Changes in the levels of inositol phosphates after agonist-dependent hydrolysis of membrane phosphoinositides. *Biochem J* **212**, 473–482.

Bradley PP, Priebat DA, Christensen RD & Rothstein G (1982). Measurement of cutaneous inflammation: estimation of neutrophil content with an enzyme marker. *J Invest Dermatol* **78**, 206–209.

Cenac N, Coelho AM, Nguyen C, Compton S, Andrade-Gordon P, MacNaughton WK, Wallace JL, Hollenberg MD, Bunnett NW, Garcia-Villar R, Bueno L & Vergnolle N (2002). Induction of intestinal inflammation in mouse by activation of proteinase-activated receptor-2. *Am J Pathol* **161**, 1903–1915.

Cenac N, Garcia-Villar R, Ferrier L, Larauche M, Vergnolle N, Bunnett NW, Coelho AM, Fioramonti J & Bueno L (2003). Proteinase-activated receptor-2-induced colonic inflammation in mice: possible involvement of afferent neurons, nitric oxide, and paracellular permeability. *J Immunol* **170**, 4296–4300.

Chin AC, Teoh DA, Scott KG, Meddings JB, Macnaughton WK & Buret AG (2002). Strain-dependent induction of enterocyte apoptosis by *Giardia lamblia* disrupts epithelial barrier function in a caspase-3-dependent manner. *Infect Immun* **70**, 3673–3680.

Corvera CU, Dery O, McConalogue K, Bohm SK, Khitin LM, Caughey GH, Payan DG & Bunnett NW (1997). Mast cell tryptase regulates rat colonic myocytes through proteinase-activated receptor 2. *J Clin Invest* **100**, 1383–1393.

Ferrier L, Mazelin L, Cenac N, Desreumaux P, Janin A, Emilie D, Colombel JF, Garcia-Villar R, Fioramonti J & Bueno L (2003). Stress-induced disruption of colonic epithelial barrier: role of interferon-gamma and myosin light chain kinase in mice. *Gastroenterology* **125**, 795–804.

Gassler N, Rohr C, Schneider A, Kartenbeck J, Bach A, Obermuller N, Otto HF & Autschbach F (2001). Inflammatory bowel disease is associated with changes of enterocytic junctions. *Am J Physiol Gastrointest Liver Physiol* **281**, G216–G228.

Gitter AH, Wullstein F, Fromm M & Schulzke JD (2001). Epithelial barrier defects in ulcerative colitis: characterization and quantification by electrophysiological imaging. *Gastroenterology* **121**, 1320–1328.

Jinguji Y & Ishikawa H (1992). Electron microscopic observations on the maintenance of the tight junction during cell division in the epithelium of the mouse small intestine. *Cell Struct Funct* **17**, 27–37.

Kong W, McConalogue K, Khitin LM, Hollenberg MD, Payan DG, Bohm SK & Bunnett NW (1997). Luminal trypsin may regulate enterocytes through proteinase-activated receptor 2. *Proc Natl Acad Sci U S A* **94**, 8884–8889.

Legoux P, Minty C, Delpech B, Minty AJ & Shire D (1992). Simultaneous quantitation of cytokine mRNAs in interleukin-1 beta stimulated U373 human astrocytoma cells by a polymerisation chain reaction method involving co-amplification with an internal multi-specific control. *Eur Cytokine Netw* **3**, 553–563.

Lindmark T, Schipper N, Lazorova L, de Boer AG & Artursson P (1998). Absorption enhancement in intestinal epithelial Caco-2 monolayers by sodium caprate: assessment of molecular weight dependence and demonstration of transport routes. *J Drug Target* **5**, 215–223.

Ma TY, Nguyen D, Bui V, Nguyen H & Hoa N (1999). Ethanol modulation of intestinal epithelial tight junction barrier. *Am J Physiol* **276**, G965–G974.

Mahraoui L, Heyman M, Plique O, Droy-Lefaix MT & Desjeux JF (1997). Apical effect of diosmectite on damage to the intestinal barrier induced by basal tumour necrosis factor-alpha. *Gut* **40**, 339–343.

Mitic LL & Anderson JM (1998). Molecular architecture of tight junctions. *Annu Rev Physiol* **60**, 121–142.

Mombaerts P, Mizoguchi E, Grusby MJ, Glimcher LH, Bhan AK & Tonegawa S (1993). Spontaneous development of inflammatory bowel disease in T cell receptor mutant mice. *Cell* **75**, 274–282.

Nguyen C, Coelho AM, Grady E, Compton SJ, Wallace JL, Hollenberg MD, Cenac N, Garcia-Villar R, Bueno L, Steinhoff M, Bunnett NW & Vergnolle N (2003). Colitis induced by proteinase-activated receptor-2 agonists is mediated by a neurogenic mechanism. *Can J Physiol Pharmacol* **81**, 920–927.

Nystedt S, Larsson AK, Aberg H & Sundelin J (1995). The mouse proteinase-activated receptor-2 cDNA and gene. Molecular cloning and functional expression. *J Biol Chem* **270**, 5950–5955.

Oshima T, Laroux FS, Coe LL, Morise Z, Kawachi S, Bauer P, Grisham MB, Specian RD, Carter P, Jennings S, Granger DN, Joh T & Alexander JS (2001). Interferon-gamma and interleukin-10 reciprocally regulate endothelial junction integrity and barrier function. *Microvasc Res* **61**, 130–143.

Pang G, Buret A, O'Loughlin E, Smith A, Batey R & Clancy R (1996). Immunologic, functional, and morphological characterization of three new human small intestinal epithelial cell lines. *Gastroenterology* **111**, 8–18.

Rodriguez P, Heyman M, Candalh C, Blaton MA & Bouchaud C (1995). Tumour necrosis factor-alpha induces morphological and functional alterations of intestinal HT29 cl. 19A cell monolayers. *Cytokine* **7**, 441–448.

Schmit A, Carol M, Robert F, Bontems P, Houben JJ, Van Gossum A, Goldman M & Mascart F (2002). Dose-effect of interleukin-10 and its immunoregulatory role in Crohn's disease. *Eur Cytokine Netw* **13**, 298–305.

Scott KG, Meddings JB, Kirk DR, Lees-Miller SP & Buret AG (2002). Intestinal infection with *Giardia* spp. reduces epithelial barrier function in a myosin light chain kinase-dependent fashion. *Gastroenterology* **123**, 1179–1190.

Streb H, Irvine RF, Berridge MJ & Schulz I (1983). Release of Ca^{2+} from a nonmitochondrial intracellular store in pancreatic acinar cells by inositol-1,4,5-trisphosphate. *Nature* **306**, 67–69.

Suenaert P, Bulteel V, Lemmens L, Noman M, Geypens B, Van Assche G, Geboes K, Ceuppens JL & Rutgeerts P (2002). Anti-tumor necrosis factor treatment restores the gut barrier in Crohn's disease. *Am J Gastroenterol* **97**, 2000–2004.

Turner JR, Rill BK, Carlson SL, Carnes D, Kerner R, Mrsny RJ & Madara JL (1997). Physiological regulation of epithelial tight junctions is associated with myosin light-chain phosphorylation. *Am J Physiol* **273**, C1378–C1385.

Yamaguchi Y, Dalle-Molle E & Hardison WG (1991). Vasopressin and A23187 stimulate phosphorylation of myosin light chain-1 in isolated rat hepatocytes. *Am J Physiol* **261**, G312–G319.

Youakim A & Ahdieh M (1999). Interferon-gamma decreases barrier function in T84 cells by reducing ZO-1 levels and disrupting apical actin. *Am J Physiol* **276**, G1279–G1288.

Zou W, Durand-Gasselin I, Dulioust A, Maillot MC, Galanaud P & Emilie D (1995). Quantification of cytokine gene expression by competitive PCR using a colorimetric assay. *Eur Cytokine Netw* **6**, 257–264.